Synthesis and biological evaluation of novel aliphatic amido-quaternary ammonium salts for anticancer chemotherapy: Part I

ARTICLE *in* EUROPEAN JOURNAL OF MEDICINAL CHEMISTRY · JULY 2011

Impact Factor: 3.45 · DOI: 10.1016/j.ejmech.2011.04.009

European Journal of Medicinal Chemistry 46 (2011) 2861–2866

Contents lists available at ScienceDirect

European Journal of Medicinal Chemistry

journal homepage: http://www.elsevier.com/locate/ejmech

Original article

Synthesis and biological evaluation of novel aliphatic amido-quaternary ammonium salts for anticancer chemotherapy: Part I

Jee Sun Yang [a], Doona Song [a], Boah Lee [a], Won Jin Ko [a], Song-Kyu Park [b], Misun Won [c], Kiho Lee [d], Hwan Mook Kim [d], Gyoonhee Han [a,e,*]

[a] Translational Research Center for Protein Function Control, Department of Biotechnology, Yonsei University, Seongsan-ro, Seodaemun-gu, Seoul 120-749, Republic of Korea
[b] College of Pharmacy, Korea University, Chochiwon, Chungnam 339-700, Republic of Korea
[c] Medical Genomics Research Center, KRIBB, Daejeon 305-806, Republic of Korea
[d] Bio-Evaluation Center, KRIBB, Ochang 363-883, Republic of Korea
[e] Department of Integrated OMICS for Biomedical Sciences (WCU Program), Yonsei University, Seoul 120-749, Republic of Korea

ARTICLE INFO

Article history:
Received 26 January 2011
Received in revised form
23 March 2011
Accepted 3 April 2011
Available online 14 April 2011

Keywords:
Aliphatic amido-quaternary ammonium salts
RhoB
GTPase RAt Sarcoma (Ras)
Perifosine
Piperazine alkyl derivatives
NSC126188

ABSTRACT

We synthesized novel aliphatic amido-quaternary ammonium salts in an effort to discover anticancer agents that increase Ras homolog gene family, member B, (RhoB) levels. These compounds exert anti-proliferative activities against several human cancer cell types. Seventeen compounds, varying in aliphatic carbon chain length and *N*-substituents, were synthesized and their biological activities were evaluated. Of these 17 compounds, compound **3i** emerged as the most promising anticancer compound by promoting apoptosis through the RhoB mediated pathway. Potent biological activities observed for these novel aliphatic amido-quaternary ammonium salt analogues support their potential as anticancer, chemotherapeutic agents.

1. Introduction

Cancer occurs when regulation of normal cell growth and differentiation is compromised due to defects in the proliferation related signaling mechanisms. Ras genes were the first-identified oncogenes, and they are observed to be mutated in 20–30% of all human tumors [1,2]. Disruption of the regulation of Ras and Ras-related proteins in cancer leads to increased invasion and metastasis, and decreased apoptosis in cancer cells. Activated Ras interacts with several effector proteins in ways that stimulate catalytic activities, and it also controls the activity of crucial signaling that regulates normal cellular proliferation [3]. Mutations in downstream targets of Ras signaling, such as v-raf murine sarcoma viral oncogene homolog B1 (B-Raf), phosphatase and tensin homolog (PTEN), and phosphatidylinositol 3-kinase (PI3K), were discovered through studies of mutated Ras [4].

Ras is a low-molecular-weight GTP/GDP binding GTPase that activates two major pathways that are deduced to play a critical role in human cancer progression [5]: 1) the PI3K/Akt pathway, and 2) the mitogen-activated Mek/extracellular signal-related kinase (Erk) pathway. Each of these pathways can induce uncontrolled proliferation and tumor cell survival by activating genes that stimulate cellular proliferation and survival. This type of carcinogenesis could be reversed in order to suppress proliferation, and/or induce apoptosis, by antagonistic effects on these two pathways.

The protein kinase B (Akt) pathway is generally activated in cancer cells and has a wide range of downstream targets that regulate tumor-associated cell processes, such as cell growth, cell cycle progression, survival, migration, epithelial–mesenchymal transition, and angiogenesis [6]. By blocking the Akt signaling pathway, apoptosis and growth inhibition in tumor cells were observed. In the last several years, a number of inhibitors of the Akt pathway have been identified by high-throughput, and virtual screening using combinatorial or medicinal chemical libraries. Phosphatidylinositol (PI) analogues are one class of Akt inhibitors

* Corresponding author. Translational Research Center for Protein Function Control, Department of Biotechnology, Yonsei University, Seongsan-ro, Seodaemun-gu, Seoul 120-749, Republic of Korea. Tel.: +82 2 21232882; fax: +82 2 3627265.
E-mail address: gyoonhee@yonsei.ac.kr (G. Han).

0223-5234/$ – see front matter © 2011 Elsevier Masson SAS. All rights reserved.
doi:10.1016/j.ejmech.2011.04.009

that is represented by perifosine [octadecyl-(1,1-dimethyl-piperidinio-4-yl)-phosphate] and phosphatidylinositol ether lipid analogues (PIAs) (Fig. 1). Perifosine is a synthetic, orally bioavailable alkylphospholipid that is structurally similar to naturally occurring phospholipids. It is known to represent a new class of antitumor agent that targets cell membranes and inhibits Akt phosphorylation, and it has exhibited significant anti-proliferative activity *in vitro* and *in vivo* in several human tumor model systems [7–11].

Not by MEK/ERK pathway but by PI3K/Akt pathway, oncogenic Ras downregulates RhoB which is a suppressor of transformation, invasion and metastasis [12]. RhoB is 86% identical at the amino acid sequence level to the RhoA-related subgroups (RhoA and RhoC), but the activities of these different proteins that relate to oncogenesis are quite different [13]. While RhoA and RhoC promote oncogenesis, invasion and metastasis, RhoB appears to be required for stress-induced apoptosis and anti-neoplastic activity, and performs as a negative moderator of cell survival [14,15]. Interestingly, it was recently reported that a piperazine alkyl derivative (NSC126188, Fig. 1), which is structurally similar to perifosine, induces apoptosis via up-regulation of RhoB in HeLa cells [16]. This prompted us to suggest that piperazine alkyl derivatives can induce apoptosis through the PI3K/Akt pathway, the RhoB mediated pathway, or both pathways.

We present the synthesis of novel aliphatic amido-quaternary ammonium salts based on the structural characteristics of lead compound NSC126188, and describe the biological activities of these derivatives. We performed a closely related structure–activity relationship (SAR) study of these compounds based on their RhoB activation using promoter assays and via assessment of anti-proliferative activities in several human cancer cell types. Our results suggest that such novel aliphatic amido-quaternary ammonium salts may be promising chemotherapeutic anticancer agents.

2. Chemistry

Based on the amidopiperazinium structure of the lead compound NSC126188, we designed and synthesized 17 analogues with two major modification points: 1) diversification of aliphatic carbon chain length, and 2) introduction of various *N*-substituents. As illustrated in Scheme 1, molecules were synthesized from the various fatty acids by two-step procedures based on design. Fatty acids **1** were reacted with thionyl chloride, and the resultant intermediate, acid chloride was amidated with 1-methylpiperazine or 1-ethylpiperazine to yield amides **2a**–**i**. Amides were converted to amido-quaternary ammonium salts (**3**) by *N*-alkylation using diverse alkyl halides. All quaternary ammonium salt analogues were fully characterized and evaluated for *in vitro* biological activities.

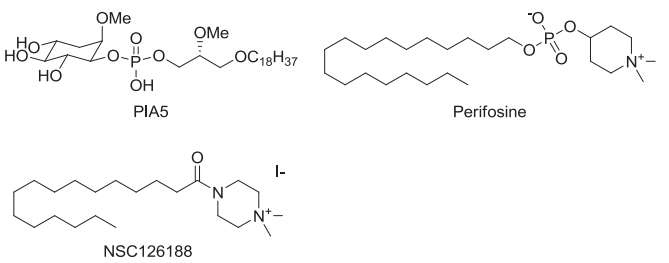

Fig. 1. Chemical structures of PI analogues (PIA5 and perifosine) and NSC126188 (4-hexadecanoyl-1,1-dimethyl-piperazin-1-ium iodide).

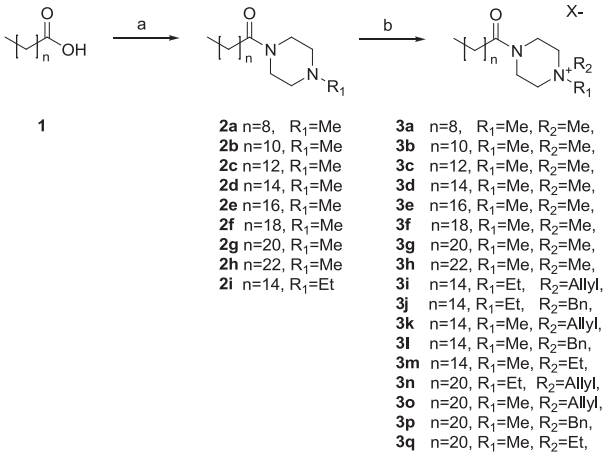

Scheme 1. Reaction protocol for the synthesis of aliphatic amido-quaternary ammonium salts (**3a**–**q**). Reagents and conditions: (a) i) $SOCl_2$, CH_2Cl_2 at 60 °C; ii) 1-alkylpiperazine, CH_2Cl_2 at 0 °C, or DMAP, EDCI, 1-alkylpiperazine, CH_2Cl_2; (b) alkyl halide, CH_3CN at ~95–100 °C or alkyl halide, toluene, ~110–115 °C.

3. Results and discussion

Compounds **3a**–**q** were assayed for growth inhibitory activity against six human cancer cell types: PC-3 (prostate cancer), NUGC-3 (gastric cancer), MDA-MB-231 (breast cancer), ACHN (renal cancer), HCT-15 (colon cancer), and NCI-H23 (non-small cell lung cancer). Results are tabulated as GI_{50} values in Tables 1–3. Perifosine, known PI3K/Akt inhibitors, and NSC126188 were each used as positive references for comparison of *in vitro* activities. Interestingly, perifosine, NSC126188, and other PI analogues share a common structural motif consisting of a long aliphatic chain and a six-membered ring. Among these known compounds, perifosine and NSC126188 also share the same amido-quaternary ammonium salt moiety with variable *N*,*N*-dimethyl substituents.

To assess the effects of carbon chain length, eight compounds with diversified chain length (from 10 to 24 carbons), were prepared. *N*,*N*-Dialkyl substituents of compounds were fixed to the dimethyl group just as the known inhibitors were. Among the eight compounds, **3c**–**f** (carbon chain length 14–20) exhibited similar levels of anti-proliferative activity. In particular, **3c** and **3f** exhibited increased growth inhibitory activity compared to perifosine and NSC126188 (re-synthesized as **3d**) in prostate cancer cell types. Compounds **3c**–**f** also showed impressive growth inhibitory activities, especially in gastric cancer cells. Compound **3d** exhibited the most potent inhibitory profiles, which were more robust than perifosine. For compounds with a relatively shorter or longer carbon chain ($n = 8$ or $n = 22$), cell growth inhibition was either observed weakly, or not observed at all, irrespective of cell type. Every compound having a carbon chain length in the range of 14–18 ($n = 12$–16) generally exhibited a more robust effect than perifosine on growth inhibition against PC-3 and NUGC-3 cell types.

On the topic of optimal chain length, we were interested in exploring the structural effects of the 6-membered ring and the *N*-alkyl substituents on potency. Therefore, carbon chain length was fixed at 16 or 22 carbons, which is same chain length of NSC126188 or perifosine, respectively. Replacements of *N*-alkyl substituents, including: methyl, ethyl, allyl, and benzyl, were investigated (**3i**–**q**). For the 16-carbon chain length series, **3i** (*N*-ethyl-*N*-allyl) exhibited remarkably potent growth inhibitory activity toward most of the human cancer cell types used in this study, except HCT-15 cell types. *N*-Methyl substituted compounds, such as **3k**, showed no activity at all. More growth inhibition tended to coincide with bulkier substituents. However, contrary to expectations benzyl

Table 1
Cell growth inhibitory activities of compounds **3a**–**h**.[a,b]

Cell line	Tissue	Growth inhibition (μM)								
		3a	**3b**	**3c**	**3d**	**3e**	**3f**	**3g**	**3h**	Perifosine
PC-3	Prostate	NA	0.58	0.29	0.48	0.53	0.31	0.99	4.79	0.44
NUGC-3	Gastric	NA	1.73	0.56	0.29	0.56	0.42	1.15	NA	0.54
MDA-MB-231	Breast	NA	3.53	0.89	1.44	1.62	1.63	3.51	NA	2.86
ACHN	Kidney	NA	NA	1.01	1.04	2.74	1.39	2.39	NA	4.56
HCT-15	Colon	NA	NA	0.85	0.58	0.81	0.54	2.41	NA	1.25
NCI-H23	Lung	NA	NA	1.58	2.34	2.7	1.74	3	NA	4.21

[a] Growth inhibition was measured by SRB (sulforhodamine B) assay.
[b] NA not active.

group substituted compounds, such as **3j** and **3l**, exhibited poor inhibitory activities. Such poor activities with benzyl group substituted compounds could be due to solubility problems. As shown in Table 4, benzyl group substituted compounds increased the log *D* value, which was calculated using Discovery Studio (Accelrys, San Diego, CA, USA).

Perifosine structural analogues having a chain length of 22 carbons ($n = 20$) were also prepared with diverse *N*-alkyl substituents. As previously stated, compounds having long carbon chains exhibit relatively poor activities (Table 1), and the overall anti-proliferative activities of **3n**–**q** were less impressive than that of perifosine. Moreover **3g**, which is strikingly similar in structure to perifosine, with the exception of the piperazine ring moiety, also exhibited poor growth inhibitory activity. It is possible that this poor level of activity is due to lipophilicity, which is supported by the A log *P*98 value. *A* log *P*98 values increase with carbon chain length. The 22-carbon chain length series is characterized by *A* log *P*98 values of 7 or greater, which is too lipophilic to reveal inhibitory activities in cellular assays. Moreover, the large number of rotatable bonds may prevent these compounds from penetrating the cell membrane. Perifosine has a relatively long carbon chain, but it has an *A* log *P*98 value of 5.75. While other compounds possess only one hydrogen bond acceptor, the carbonyl group adjacent to the piperazine ring, perifosine has four hydrogen bond acceptors, and this might impact the *A* log *P*98 value in a way that counter balances the effect of the long carbon chain (Table 4).

Based on the results of the RhoB promoter assay, the anti-proliferative activity of the prepared analogues parallels their ability to induce reporter output (Fig. 2). For the first compound set (**3a**–**h**), molecules with potent anti-proliferative activities robustly induced reporter expression in the RhoB promoter-based assay. For example, compounds **3c**, **3d** and **3f** exhibited potent anti-proliferative activity and showed the ability to induce reporter expression in the RhoB promoter-based assay, while other compounds (**3a**, **3b**, **3g**, and **3h**) with poor anti-proliferative activities exhibited poor ability to induce reporter expression through the RhoB promoter. This result suggests that cell growth inhibition is decreased by apoptosis, which can be induced by activated RhoB after the treatment with these analogues.

In the series of diverse *N*-alkyl substituted compounds (**3i**–**m**) that have 16 carbon chains, anti-proliferative activities against both prostate and gastric cancer cell types were observed. Similarly, corresponding RhoB promoter-based reporter expression levels were generally high. The *N*-ethyl-*N*-allyl substituted compound **3i** exhibited the most robust reporter induction and the most impressive overall growth inhibitory effects. The same *N*-ethyl-*N*-allyl substituted characteristic in the context of the 22-carbon chain compounds resulted in similar ability to induce reporter gene expression. However, **3k** (*N*-methyl-*N*-allyl) lacked anti-proliferative activities, but induced reporter levels quite highly. This may indicate that some compounds, including **3k**, mediate other signaling pathways that offset the regulation of apoptosis by RhoB. As mentioned above, compounds with 22-carbon chain length are highly lipophilic that the compounds are hardly dissolved to penetrate cell membranes. Thus, the compounds showed conspicuously low RhoB expression level, except **3n** which has *N*-ethyl-*N*-allyl substituent same as the most potent analogue, **3i**.

The substituent effect may be explained through comparison of the differences in reporter levels versus anti-proliferative activity between three sets of compounds: 1) comparison of **3i** (*N*-ethyl-*N*-allyl) to **3d** (*N*,*N*-dimethyl), 2) comparison of **3n** (*N*-ethyl-*N*-allyl) to **3g** (*N*,*N*-dimethyl), and 3) comparison of **3n** to perifosine (*N*,*N*-dimethyl). Based on the reporter outputs for first two sets of compounds, *N*-ethyl-*N*-allyl substituted analogues exhibited almost twice the reporter induction ability of that observed from *N*,*N*-dimethyl substituted compounds. The last set of compounds (**3n** compared with perifosine) illustrated similar levels of induction control. In regards to effects on cell growth, **3i** showed greater anti-proliferative activities than **3d** in human cancer cell types, and these activities are in conjunction with reporter induction through the RhoB promoter. The growth inhibitory activity of **3n**, however, was inferior to that of perifosine, even though they induce similar levels of reporter expression through the RhoB promoter. Such results could be also explained by the lipophilic properties of these compounds, as mentioned above. While carbon chain length in these compounds is the same, the lipophilicity of perifosine could be offset by four hydrogen bond acceptors. Consequently, perifosine might be more soluble *in vitro* and more easily access the

Table 2
Cell growth inhibitory activities of compounds **3i**–**m**.

Cell line	Tissue	Growth inhibition (μM)						
		3i	**3j**	**3k**	**3l**	**3m**	**3d**	Perifosine
PC-3	Prostate	0.37	0.55	NA	0.51	0.8	0.48	0.44
NUGC-3	Gastric	0.27	0.46	NA	1	0.58	0.29	0.54
MDA-MB-231	Breast	0.68	1.16	NA	1.45	2.05	1.44	2.86
ACHN	Kidney	0.5	0.92	NA	1.98	1.89	1.04	4.56
HCT-15	Colon	1.33	NA	NA	5.06	1.8	0.58	1.25
NCI-H23	Lung	0.88	1.76	NA	2.05	3.65	2.34	4.21

Table 3
Cell growth inhibitory activities of compounds **3n**–**q**.

Cell line	Tissue	Growth inhibition (μM)					
		3n	**3o**	**3p**	**3q**	**3g**	Perifosine
PC-3	Prostate	1.47	0.96	1.24	0.85	0.99	0.44
NUGC-3	Gastric	1.54	1.53	1.9	1.22	1.15	0.54
MDA-MB-231	Breast	2.53	3.16	1.98	2.01	3.51	2.86
ACHN	Kidney	3.38	2.37	4.74	1.9	2.39	4.56
HCT-15	Colon	2.78	2.13	2.53	1.69	2.41	1.25
NCI-H23	Lung	3.94	3.07	2.95	2.6	3	4.21

Table 4
Molecular properties of compounds **3a**–**q**.

	A log *P*98	log *D*	Num_rotatable bonds	Num_H _acceptors	Num_H _donors
3a	2.042	−1.070	8	1	0
3b	2.954	−0.158	10	1	0
3c	3.867	0.755	12	1	0
3d	4.779	1.667	14	1	0
3e	5.692	2.579	16	1	0
3f	6.604	3.492	18	1	0
3g	7.516	4.404	20	1	0
3h	8.429	5.317	22	1	0
3i	5.745	3.327	17	1	0
3j	6.712	4.294	17	1	0
3k	5.396	2.978	16	1	0
3l	6.363	3.945	16	1	0
3m	5.128	2.016	15	1	0
3n	8.482	6.064	23	1	0
3o	8.133	5.715	22	1	0
3p	9.100	6.682	22	1	0
3q	7.865	4.753	21	1	0
Perifosine	5.750	4.607	20	4	0

surface of the cell membrane than **3n**, thereby facilitating an ability to penetrate the membrane.

Perifosine inhibits PI3K/Akt, and NSC126188 modulates RhoB. These two compounds exhibit structural similarities that may be responsible for regulating apoptosis through PI3K/Akt pathway and/or RhoB mediated pathways. Therefore, we have designed and synthesized 17 aliphatic amido-quaternary ammonium salts for anticancer chemotherapeutic agents based on the structural moieties common to both compounds. We then evaluated the effects of diversity in carbon chain length and *N*-substituent patterns on the growth of six human cancer cell types. Compound **3i** emerged as the most promising anticancer agent, exhibiting potent inhibition of cancer cell growth and stimulation of apoptosis. The effects of **3i** in RhoB promoter-based reporter assays indicate that this compound may act through RhoB mediated signaling. Compound **3i** showed impressive parallels in activities based on the ability to prevent cell proliferation by gastric and prostate cancer cells and the ability to induce reporter output in the RhoB promoter-based assay. This study is the first to identify aliphatic amido-quaternary ammonium salts that have potential chemotherapeutic properties and act through the RhoB mediated pathway.

4. Experimental section

All chemicals were obtained from commercial suppliers and used without further purification. All reactions were monitored by thin layer chromatography (TLC) on precoated silica gel 60 F_{254} (mesh) (E. Merck, Mumbai, India) and spots were visualized under UV light (254 nm). Flash column chromatography was performed with silica (Merck EM9385, 230–400 mesh). ^{1}H nuclear magnetic resonance (NMR; Varian) spectra were recorded at 300 and 75 MHz, at 400 and 100 MHz, or at 500 and 125 MHz. Proton and carbon chemical shifts are expressed in parts per million relative to internal tetramethylsilane, and coupling constants (*J*) are expressed in hertz. Liquid chromatography/mass spectrometry (LC/MS) spectra were recorded by electrospray ionization (ESI) on Shimadzu LC/MS instruments (10% 0.1% TFA in H_2O/90% 0.1% TFA in acetonitrile) scan (from 0 to 600 amu/*z*) mode, and the detected ion peaks are $(M^+z)/z$ and $(M^-z)/z$ in positive and negative ion modes, respectively, where M represents the molecular weight of the compound and *z* represents the charge (number of protons). High resolution mass spectrometry (HRMS) spectra were obtained from fast atom bombardment (FAB) on the JMS-700 (Jeol, Japan) High Resolution Tandem Mass Spectrometer at the Korea Basic Science Institute in Seoul, Korea.

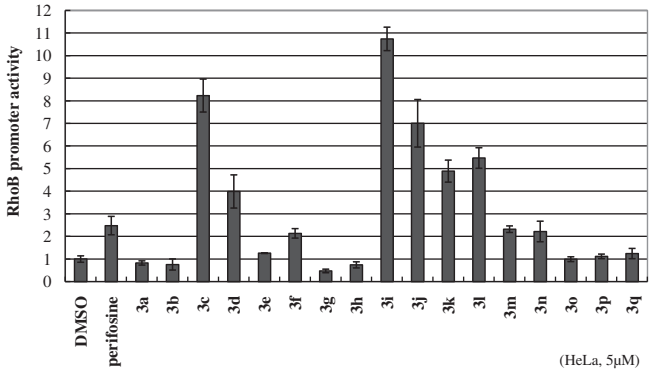

Fig. 2. Detection of RhoB promoter activation by reporter assay. Luciferase activity was determined in the cells transfected with either the pGL2 vector or pGL-RhoB-Luc in the presence of aliphatic amido-quaternary ammonium salts.

4.1. Procedures for ***2a–i***

Fatty acid **1** (2.9 mmol) was dissolved in anhydrous dichloromethane (0.1 M solution), and then thionyl chloride (3.0 equiv) was added under argon (Ar) atmosphere. The stirred suspension was heated to reflux for 4 h. Then the reaction mixture was cooled and poured onto crushed ice for 1 h. Piperazine (5.8 mmol) was added dropwise, and the reaction mixture was then allowed to warm up to room temperature and stirred for 2 h. NaOH solution (10%) was added (final pH 13), and the mixture was extracted with chloroform. The organic layer was washed with brine, dried over anhydrous $MgSO_4$, and then concentrated *in vacuo*. The residue was purified by chromatography on silica gel with 5% MeOH/$CHCl_3$ to afford the corresponding amides.

General procedures 1 (amidation step in Scheme 1)

Carboxylic acid **1** (2.9 mmol) was dissolved in anhydrous dichloromethane (0.2 M) at room temperature under Ar atmosphere. Piperazine (4.3 mmol), EDC (1-ethyl-3-[3-dimethylaminopropyl] carboimide hydrochloride, 4.3 mmol) and DMAP (4-dimethylaminopyridine, 0.9 mmol) were added, and the mixture was stirred for 8 h at room temperature. Saturated NH_4Cl solution was added, and the mixture was extracted with dichloromethane (3×). The organic layer was washed with brine, dried over anhydrous Na_2SO_4, and concentrated *in vacuo*. The residue was purified by chromatography on silica gel with 5% MeOH/CH_2Cl_2 to afford amides.

4.1.1. 1-(4-Methylpiperazin-1-yl)decan-1-one (***2a***)

^{1}H NMR ($CDCl_3$, 500 MHz) δ 3.65–3.58 (m, 2H), 3.51–3.45 (m, 2H), 2.46–2.36 (m, 4H), 2.30 (s, 3H), 2.23 (t, $J = 7.5$ Hz, 2H), 1.57–1.50 (m, 2H), 1.35–1.10 (m, 12H), 0.80 (t, $J = 6.7$ Hz, 3H); ESI-MS: $m/z = 255$ [M^+H].

4.1.2. 1-(4-Methylpiperazin-1-yl)dodecan-1-one (***2b***)

^{1}H NMR ($CDCl_3$, 300 MHz) δ 3.72–3.67 (m, 2H), 3.53 (t, $J = 4.5$ Hz, 2H), 2.50–2.41 (m, 4H), 2.36 (s, 3H), 2.30 (t, $J = 7.8$ Hz, 2H), 1.65–1.54 (m, 2H), 1.36–1.22 (m, 16H), 0.87 (t, $J = 6.6$ Hz, 3H); ESI-MS: $m/z = 283$ [M^+H].

4.1.3. 1-(4-Methylpiperazin-1-yl)tetradecan-1-one (***2c***)

^{1}H NMR ($CDCl_3$, 500 MHz) δ 3.65–3.55 (m, 2H), 3.46 (t, $J = 4.5$ Hz, 2H), 2.39 (t, $J = 5.0$ Hz, 4H), 2.29 (s, 3H), 2.23 (t, $J = 5.0$ Hz, 2H), 1.57–1.51 (m, 2H), 1.28–1.13 (m, 20H), 0.80 (t, $J = 6.7$ Hz, 3H); ESI-MS: $m/z = 311$ [M^+H].

*4.1.4. 1-(4-Methylpiperazin-1-yl)hexadecan-1-one (**2d**)*

^{1}H NMR (DMSO-d_6, 500 MHz) δ 3.96–3.84 (m, 4H), 3.17 (m, 4H), 2.68 (s, 3H), 2.31 (t, J = 7.5 Hz, 2H), 1.64–1.58 (m, 2H), 1.29–1.21 (m, 24H), 0.87 (t, J = 7.0 Hz, 3H); ESI-MS: m/z = 339 [M$^+$H].

*4.1.5. 1-(4-Methylpiperazin-1-yl)octadecan-1-one (**2e**)*

^{1}H NMR ($CDCl_3$, 400 MHz) δ 3.63 (t, J = 4.8 Hz, 2H), 3.47 (t, J = 4.8 Hz, 2H), 2.41–2.35 (m, 4H), 2.30 (t, J = 8.0 Hz, 5H), 1.64–1.59 (m, 2H), 1.34–1.23 (m, 28H), 0.88 (t, J = 6.8 Hz, 3H); ESI-MS: m/z = 367 [M$^+$H].

*4.1.6. 1-(4-Methylpiperazin-1-yl)icosan-1-one (**2f**)*

^{1}H NMR ($CDCl_3$, 300 MHz) δ 3.72 (br m, 2H), 3.58–3.55 (m, 2H), 2.51–2.49 (m, 4H), 2.40 (s, 3H), 2.32 (t, J = 7.7 Hz, 2H), 1.65–1.60 (m, 2H), 1.30–1.26 (m, 32H), 0.89 (t, J = 6.7 Hz, 3H); ESI-MS: m/z = 395 [M$^+$H].

*4.1.7. 1-(4-Methylpiperazin-1-yl)docosan-1-one (**2g**)*

^{1}H NMR ($CDCl_3$, 400 MHz) δ 3.64 (t, J = 5.0 Hz, 2H), 3.48 (t, J = 5.0 Hz, 2H), 2.41–2.36 (m, 4H), 2.33 (t, J = 7.8 Hz, 5H), 1.65–1.58 (m, 2H), 1.30–1.25 (m, 36H), 0.88 (t, J = 6.8 Hz, 3H); ESI-MS: m/z = 423 [M$^+$H].

*4.1.8. 1-(4-Methylpiperazin-1-yl)tetracosan-1-one (**2h**)*

^{1}H NMR ($CDCl_3$, 300 MHz) δ 3.75 (br m, 2H), 3.60 (m, 2H), 2.55 (m, 4H), 2.43 (s, 3H), 2.32 (t, J = 7.6 Hz, 2H), 1.65–1.58 (m, 2H), 1.31–1.20 (m, 40H), 0.89 (t, J = 6.6 Hz, 3H); ESI-MS: m/z = 451 [M$^+$H].

*4.1.9. 1-(4-Ethylpiperazin-1-yl)hexadecan-1-one (**2i**)*

^{1}H NMR (CD_3OD, 500 MHz) δ 3.62–3.57 (m, 4H), 2.51–2.44 (m, 6H), 2.39 (t, J = 7.7 Hz, 2H), 1.59 (br m, 2H), 1.33–1.29 (m, 24H), 1.13 (t, J = 7.2 Hz, 3H), 0.91 (t, J = 7.0 Hz, 3H); ESI-MS: m/z = 353 [M$^+$H].

*4.2. Procedures for **3a–q***

Alkyl halide (1.6 mmol) was added to a solution of **2a–i** (0.8 mmol) in anhydrous acetonitrile (0.3 M) at room temperature. Then, the reaction mixture was heated to ~140–150 °C for 7 h. After the reaction mixture equilibrated to room temperature, the precipitate was granulated for 1 h at 0 °C. Solids were collected by filtration, washed with ethyl acetate, and dried *in vacuo*.

*4.2.1. 4-Decanoyl-1,1-dimethylpiperazin-1-ium iodide (**3a**)*

^{1}H NMR (DMSO-d_6, 300 MHz) δ 3.78–3.75 (m, 4H), 3.40–3.34 (m, 4H), 3.12 (s, 6H), 2.32 (t, J = 7.2 Hz, 2H), 1.50–1.42 (m, 2H), 1.30–1.21 (m, 12H), 0.85 (t, J = 6.6 Hz, 3H); MS (FAB) m/z 269(MH$^+$). HRMS (FAB) calcd. for $C_{16}H_{33}N_2OI$ (MH$^+$) 269.2593, found 269.2600.

*4.2.2. 4-Dodecanoyl-1,1-dimethylpiperazin-1-ium iodide (**3b**)*

^{1}H NMR ($CDCl_3$, 300 MHz) δ 4.02–3.83 (m, 5H), 3.65–3.55 (m, 8H), 2.39 (t, J = 7.5 Hz, 2H), 1.68–1.55 (m, 5H), 1.36–1.22 (m, 16H), 0.87 (t, J = 6.6 Hz, 3H); ^{13}C NMR (DMSO-d_6, 500 MHz) δ 171.78, 60.91, 60.91, 60.76, 55.26, 51.16, 46.58, 40.48, 39.72, 29.75, 29.42, 25.23, 22.80, 14.67; MS (FAB) m/z 297 (MH$^+$). HRMS (FAB) calcd. for $C_{18}H_{37}N_2OI$ (MH$^+$) 297.2906, found 297.2908.

*4.2.3. 1,1-Dimethyl-4-tetradecanoylpiperazin-1-ium iodide (**3c**)*

^{1}H NMR (DMSO-d_6, 300 MHz) δ 3.76 (s, 4H), 3.39–3.34 (m, 4H), 3.12 (s, 6H), 2.31 (t, J = 7.2 Hz, 2H), 1.50–1.41 (m, 2H), 1.30–1.20 (m, 20H), 0.83 (t, J = 6.6 Hz, 3H); MS (FAB) m/z 325 (MH$^+$). HRMS (FAB) calcd. for $C_{20}H_{41}N_2OI$ (MH$^+$) 325.3219, found 325.3224.

*4.2.4. 1,1-Dimethyl-4-palmitoylpiperazin-1-ium iodide (**3d**)*

^{1}H NMR (DMSO-d_6, 500 MHz) δ 3.79–3.76 (m, 4H), 3.41–3.39 (m, 4H), 3.14 (s, 6H), 2.34 (t, J = 7.5 Hz, 2H), 1.49–1.47 (m, 2H), 1.26–1.24 (br m, 24H), 0.85 (t, J = 7.0 Hz, 3H); ^{13}C NMR (DMSO-d_6, 500 MHz) δ 171.76, 60.90, 60.76, 51.1, 40.39, 39.73, 32.00, 29.72, 29.42, 25.24, 22.80, 14.66; MS (FAB) m/z 353 (MH$^+$), HRMS (FAB) calcd. for $C_{22}H_{45}N_2OI$ (MH$^+$) 353.3532, found 353.3537.

*4.2.5. 1,1-Dimethyl-4-stearoylpiperazin-1-ium iodide (**3e**)*

^{1}H NMR (DMSO-d_6, 400 MHz) δ 3.77 (t, J = 5.4 Hz, 4H), 3.39 (t, J = 4.8 Hz, 2H), 3.32–3.30 (m, 2H), 3.14 (s, 6H), 2.33 (t, J = 7.2 Hz, 2H), 1.50–1.45 (m, 2H), 1.25–1.20 (m, 28H), 0.85 (t, J = 5.6 Hz, 3H); ^{13}C NMR (DMSO-d_6, 500 MHz) δ 171.72, 62.31, 60.96, 60.83, 51.22, 40.45, 39.79, 31.99, 29.74, 29.40, 25.23, 22.78, 14.62; MS (FAB) m/z 381 (MH+). HRMS (FAB) calcd. for $C_{24}H_{49}N_2OI$ (MH$^+$) 381.3845, found 381.3843.

*4.2.6. 4-Icosanoyl-1,1-dimethylpiperazin-1-ium iodide (**3f**)*

^{1}H NMR (DMSO-d_6, 400 MHz) δ 3.78 (m, 4H), 3.39 (m, 4H), 3.14 (s, 6H), 2.33 (t, J = 7.6 Hz, 2H), 1.48 (m, 2H), 1.23 (m, 32H), 0.85 (t, J = 6.4 Hz, 3H); MS (FAB) m/z 409 (MH$^+$). HRMS (FAB) calcd. for $C_{26}H_{53}N_2O$ I (MH$^+$) 409.4158, found 409.5097.

*4.2.7. 4-Docosanoyl-1,1-dimethylpiperazin-1-ium iodide (**3g**)*

^{1}H NMR (DMSO-d_6, 300 MHz) δ 3.76 (br, 4H), 3.37 (br, 4H), 3.12 (s, 6H), 2.32 (t, J = 7.4 Hz, 2H), 1.43 (m, 2H), 1.22 (m, 36H), 0.84 (t, J = 5.9 Hz, 3H); MS (FAB) m/z 437 (MH$^+$). HRMS (FAB) calcd. for $C_{28}H_{57}N_2OI$ (MH$^+$) 437.4471, found 437.4470.

*4.2.8. 1,1-Dimethyl-4-tetracosanoylpiperazin-1-ium iodide (**3h**)*

^{1}H NMR (DMSO-d_6, 300 MHz) δ 3.69(m, 4H), 3.26 (m, 4H), 3.06 (s, 6H), 2.25 (t, J = 7.3 Hz, 2H), 1.39 (m, 2H), 1.14 (m, 40H), 0.76 (t, J = 6.0 Hz, 3H); ^{13}C NMR (DMSO-d_6, 500 MHz) δ 171.82, 61.05, 51.53, 51.20, 40.59, 40.25, 39.92, 32.66, 29.64, 29.32, 25.22, 22.72, 14.54; MS (FAB) m/z 465 (MH$^+$). HRMS (FAB) calcd. for $C_{30}H_{61}N_2OI$ (MH$^+$) 465.4784, found 465.4783.

4.2.9. 1-Allyl-1-ethyl-4-palmitoylpiperazin-1-ium bromide (3i)

^{1}H NMR (DMSO-d_6, 500 MHz) δ 6.04–5.97 (m, 1H), 5.71–5.63 (m, 2H), 4.08 (d, J = 7.5 Hz, 2H), 3.80–3.77 (m, 4H), 3.44–3.38 (m, 4H), 3.36–3.35 (m, 2H), 2.34 (t, J = 7.5 Hz, 2H), 1.50–1.47 (m, 2H), 1.26–1.24 (br m, 27H), 0.85 (t, J = 7.0 Hz, 3H); ^{13}C NMR (DMSO-d_6, 500 MHz) δ 171.84, 128.27, 125.78, 59.45, 57.17, 57.00, 54.12, 40.47, 39.87, 32.61, 29.72, 29.41, 25.19, 22.80, 14.67, 7.55; MS (FAB) m/z 393 (MH$^+$). HRMS (FAB) calcd. for $C_{25}H_{49}N_2OBr$ (MH$^+$) 393.3845, found 393.3847.

*4.2.10. 1-Benzyl-1-ethyl-4-palmitoylpiperazin-1-ium bromide (**3j**)*

^{1}H NMR (DMSO-d_6, 500 MHz) δ 7.56–7.52 (m, 5H), 4.64 (s, 2H), 4.13–4.09 (m, 1H), 3.97–3.94 (m, 1H), 3.74–3.71 (m, 1H), 3.54–3.49 (m, 1H), 3.40–3.36 (m, 4H), 3.30–3.27 (m, 2H), 2.36–2.30 (m, 2H), 1.49–1.46 (m, 2H), 1.37 (t, J = 7.2 Hz, 3H), 1.24–1.20 (br m, 24H), 0.85 (t, J = 7.5 Hz, 3H); ^{13}C NMR (DMSO-d_6, 500 MHz) δ 171.84, 133.68, 131.07, 129.74, 127.91, 62.55, 56.09, 51.64, 40.55, 35.36, 29.72, 29.41, 25.17, 22.80, 14.67, 9.87, 7.91; MS (FAB) m/z 443 (MH$^+$). HRMS (FAB) calcd. for $C_{29}H_{51}N_2OBr$ (MH$^+$) 443.4001, found 443.3998.

*4.2.11. 1-Allyl-1-methyl-4-palmitoylpiperazin-1-ium bromide (**3k**)*

^{1}H NMR (DMSO-d_6, 500 MHz) δ 6.10–6.02 (m, 1H), 5.66 (d, J = 12.5 Hz, 2H), 4.10 (d, J = 7.5 Hz, 2H), 3.94–3.86 (m, 2H), 3.77–3.74 (m, 1H), 3.65–3.62 (m, 1H), 3.39–3.37 (m, 4H), 3.07 (s, 3H), 2.34 (t, J = 7.5 Hz, 2H), 1.49–1.47 (m, 2H), 1.24 (br m, 24H), 0.85 (t, J = 6.8 Hz, 3H); ^{13}C NMR (DMSO-d_6, 500 MHz) δ 171.80, 156.23, 128.75, 125.94, 65.24, 59.00, 47.06, 40.64, 40.21, 39.29, 29.77, 29.42,

25.23, 22.80, 14.66; MS (FAB) *m/z* 379 (MH^+). HRMS (FAB) calcd. for $C_{24}H_{47}N_2O$ Br (MH^+) 379.3688, found 379.3695.

*4.2.12. 1-Benzyl-1-methyl-4-palmitoylpiperazin-1-ium bromide (**3l**)*

^{1}H NMR (DMSO-d_6, 500 MHz) δ 7.56–7.53 (m, 5H), 4.66 (s, 2H), 4.20–4.17 (m, 1H), 4.01–3.98 (m, 1H), 3.73–3.69 (m, 2H), 3.49–3.48 (m, 2H), 3.39–3.37 (m, 2H), 3.02 (s, 3H), 2.35 (q, $J = 7.5$ Hz, 2H), 1.50–1.47 (m, 2H), 1.27–1.24 (br m, 24H), 0.85 (t, $J = 7.0$ Hz, 3H); ^{13}C NMR (DMSO-d_6, 500 MHz) δ 171.78, 133.89, 131.04, 129.61, 128.02, 67.44, 59.23, 59.01, 45.46, 40.21, 39.41, 32.63, 29.78, 29.43, 25.23, 22.81, 14.66; MS (FAB) *m/z* 429 (MH^+). HRMS (FAB) calcd. for $C_{28}H_{49}N_2OBr$ (MH^+) 429.3845, found 429.3846.

*4.2.13. 1-Ethyl-1-methyl-4-palmitoylpiperazin-1-ium iodide (**3m**)*

^{1}H NMR (DMSO-d_6, 500 MHz) δ 3.95–3.84 (m, 2H), 3.75–3.71 (m, 1H), 3.60–3.56 (m, 1H), 3.46 (q, $J = 7.0$ Hz, 4H), 3.40 (m, 2H), 3.06 (s, 3H), 2.34 (t, $J = 7.5$ Hz, 2H), 1.49–1.47 (m, 2H), 1.26–1.20 (br m, 27H), 0.85 (t, $J = 7.0$ Hz, 3H); ^{13}C NMR (DMSO-d_6, 500 MHz) δ 171.75, 59.28, 59.13, 58.81, 45.99, 40.41, 39.34, 35.49, 29.79, 29.64, 29.44, 25.22, 22.81, 14.85, 7.84; MS (FAB) *m/z* 367 (MH^+). HRMS (FAB) calcd. for $C_{23}H_{47}N_2OI$ (MH^+) 367.3688, found 367.3690.

*4.2.14. 1-Allyl-4-docosanoyl-1-ethylpiperazin-1-ium bromide (**3n**)*

^{1}H NMR ($CDCl_3$, 300 MHz) δ 5.90–6.00 (m, 2H), 5.76–5.80 (m, 1H), 4.46 (br, 2H), 3.74–4.01 (br, 6H), 3.63–3.72 (m, 2H), 3.53–3.57 (br, 2H), 2.36 (t, $J = 7.6$ Hz, 2H), 1.54–1.61 (m, 2H), 1.49 (t, $J = 7.3$ Hz, 3H), 1.23 (br, 36H), 0.86 (t, $J = 6.6$ Hz, 3H); MS (FAB) *m/z* 477 (MH^+). HRMS (FAB) calcd. for $C_{31}H_{61}N_2OBr$ (MH^+) 477.4784, found 477.4785.

*4.2.15. 1-Allyl-4-docosanoyl-1-methylpiperazin-1-ium bromide (**3o**)*

^{1}H NMR (DMSO-d_6, 300 MHz) δ 6.03 (m, 1H), 5.66 (m, 2H), 4.09 (d, $J = 7.2$ Hz, 2H), 3.59–3.94 (m, 4H), 3.33–3.37 (m, 4H), 3.06 (s, 3H), 2.34 (t, $J = 7.4$ Hz, 2H), 1.46 (m, 2H), 1.21 (s, 36H), 0.83 (t, $J = 6.1$ Hz, 3H); MS (FAB) *m/z* 463 (MH^+). HRMS (FAB) calcd. for $C_{30}H_{59}N_2OBr$ (MH^+) 463.4627, found 463.4626.

*4.2.16. 1-Benzyl-4-docosanoyl-1-methylpiperazin-1-ium bromide (**3p**)*

^{1}H NMR (DMSO-d_6, 300 MHz) δ 7.53 (m, 5H), 4.66 (s, 2H), 3.66–4.19 (m, 4H), 3.41–3.46 (m, 4H), 3.01 (s, 3H), 2.32 (br, 2H), 1.47 (br, 2H), 1.22 (m, 36H), 0.83 (t, $J = 6.3$ Hz, 3H); ^{13}C NMR (DMSO-d_6, 500 MHz) δ 171.88, 128.78, 125.91, 64.72, 59.31, 47.28, 40.41, 40.24, 40.08, 39.91, 35.52, 31.94, 29.32, 25.21, 22.72, 14.54; MS (FAB) *m/z* 513 (MH^+). HRMS (FAB) calcd. for $C_{34}H_{61}N_2OBr$ (MH^+) 513.4784, found 513.4786.

*4.2.17. 4-Docosanoyl-1-ethyl-1-methylpiperazin-1-ium iodide (**3q**)*

^{1}H NMR ($CDCl_3$, 300 MHz) δ 3.53–4.20 (m, 8H), 3.47 (s, 3H), 2.36 (t, $J = 7.4$ Hz, 2H), 1.46–1.62 (m, 5H), 1.24 (br, 36H), 0.85 (t, $J = 7.0$ Hz, 3H); ^{13}C NMR (DMSO-d_6, 500 MHz) δ 171.82, 133.88, 131.07, 129.64, 127.98, 67.88, 67.72, 59.33, 45.85, 45.64, 40.43, 39.93, 35.73, 29.68, 29.33, 25.21, 22.72, 14.54; MS (FAB) *m/z* 451 (MH^+). HRMS (FAB) calcd. for $C_{29}H_{59}N_2OI$ (MH^+) 451.4627, found 451.4626.

4.3. Sulforhodamine (SRB) assay

Growth inhibition of cancer cell lines in the presence of NSC126188 was determined using the SRB assay, as previously described [17]. SRB dye bound to the cell matrix was quantified using a spectrophotometer at 530 nm.

4.4. Luciferase assay

Transactivation of RhoB was determined by reporter assay using the dual-luciferase reporter assay system (Promega, Madison, WI, USA), as previously described [18]. HeLa cells at 75–90% confluence were transiently cotransfected with the pGL2-RhoB-firefly luciferase plasmid containing the RhoB promoter, and pRL-SV40-renilla luciferase. Luciferase activity was integrated over a 10-s period and measured using a luminometer (Victor X Light; Perkin Elmer, Waltham, MA, USA). The results were normalized to the levels of renilla luciferase.

Acknowledgments

This research was supported by the 21st Century Frontier for Functional Analysis of the Human Genome, National Research Foundation (2009-0092966), Korean Research WCU Grant (R31-2008-000-10086-0) and the Brain Korea 21 Project, of the Republic of Korea.

References

[1] J.L. Bos, Ras oncogenes in human cancer: a review, Cancer Res. 49 (1989) 4682–4689.
[2] M. Malumbres, M. Barbacid, RAS oncogenes: the first 30 years, Nat. Rev. Cancer 3 (2003) 459–465.
[3] J. Downward, Targeting RAS signalling pathways in cancer therapy, Nat. Rev. Cancer 3 (2003) 11–22.
[4] P. Rodriguez-Viciana, O. Tetsu, K. Oda, J. Okada, K. Rauen, F. McCormick, Cancer targets in the Ras Pathway, Cold Spring Harb. Symp. Quant. Biol. 70 (2005) 461–467.
[5] A.D. Cox, C.J. Der, Ras family signaling: therapeutic targeting, Cancer Biol. Ther. 1 (2002) 599–606.
[6] C.W. Lindsley, The Akt/PKB family of protein kinases: a review of small molecule inhibitors and progress towards target validation: a 2009 update, Curr. Top. Med. Chem. 10 (2010) 458–477.
[7] S.B. Kondapaka, S.S. Singh, G.P. Dasmahapatra, E.A. Sausville, K.K. Roy, Perifosine, a novel alkylphospholipid, inhibits protein kinase B activation, Mol. Cancer Ther. 2 (2003) 1093–1103.
[8] G.A. Ruiter, S.F. Zerp, H. Bartelink, W.J. van Blitterswijk, M. Verheij, Anti-cancer alkyl-lysophospholipids inhibit the phosphatidylinositol 3-kinase-Akt/PKB survival pathway, Anticancer Drugs 14 (2003) 167–173.
[9] A.M. Senderowicz, Small-molecule cyclin-dependent kinase modulators, Oncogene 22 (2003) 6609–6620.
[10] A.M. Senderowicz, Novel direct and indirect cyclin-dependent kinase modulators for the prevention and treatment of human neoplasms, Cancer Chemother. Pharmacol. 52 (Suppl. 1) (2003) S61–S73.
[11] S.R. Vink, J.H. Schellens, W.J. van Blitterswijk, M. Verheij, Tumor and normal tissue pharmacokinetics of perifosine, an oral anti-cancer alkylphospholipid, Invest. New Drugs 23 (2005) 279–286.
[12] K. Jiang, J. Sun, J. Cheng, J.Y. Djeu, S. Wei, S. Sebti, Akt mediates Ras down-regulation of RhoB, a suppressor of transformation, invasion, and metastasis, Mol. Cell. Biol. 24 (2004) 5565–5576.
[13] A.P. Wheeler, A.J. Ridley, Why three Rho proteins? RhoA, RhoB, RhoC, and cell motility, Exp. Cell Res. 301 (2004) 43–49.
[14] A.J. Ridley, Rho proteins and cancer, Breast Cancer Res. Treat. 84 (2004) 13–19.
[15] M. Wu, Z.F. Wu, C. Kumar-Sinha, A. Chinnaiyan, S.D. Merajver, RhoC induces differential expression of genes involved in invasion and metastasis in MCF10A breast cells, Breast Cancer Res. Treat. 84 (2004) 3–12.
[16] B.K. Kim, D.M. Kim, K.S. Chung, S.K. Park, S.J. Choi, A. Song, K. Lee, C.W. Lee, K.B. Song, G. Han, J. Simon, H.M. Kim, M. Won, NSC126188, a piperazine alkyl derivative, induces apoptosis via upregulation of RhoB in HeLa cells, Invest. New Drugs (2010).
[17] D.M. Kim, S.Y. Koo, K. Jeon, M.H. Kim, J. Lee, C.Y. Hong, S. Jeong, Rapid induction of apoptosis by combination of flavopiridol and tumor necrosis factor (TNF)-alpha or TNF-related apoptosis-inducing ligand in human cancer cell lines, Cancer Res. 63 (2003) 621–626.
[18] M.S. Won, N. Im, S. Park, S.K. Boovanahalli, Y. Jin, X. Jin, K.S. Chung, M. Kang, K. Lee, S.K. Park, H.M. Kim, B.M. Kwon, J.J. Lee, A novel benzimidazole analogue inhibits the hypoxia-inducible factor (HIF)-1 p.thway, Biochem. Biophys. Res. Commun. 385 (2009) 16–21.